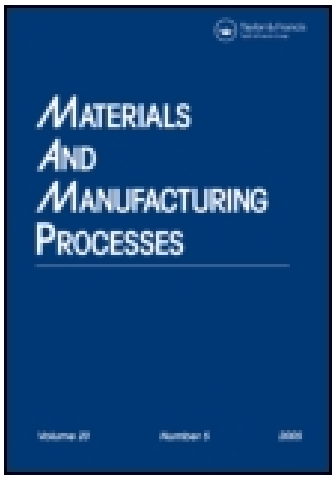

Materials and Manufacturing Processes
Publication details, including instructions for authors and subscription information:
http://www.tandfonline.com/loi/lmmp20

Laser Lap Joining of Dissimilar Materials: A Review of Factors Affecting Joint Strength

K. F. Tamrin [a b], Y. Nukman [a] & S. S. Zakariyah [b c]

[a] Department of Mechanical Engineering, Faculty of Engineering , University of Malaya , Kuala Lumpur , Malaysia

[b] Advanced Technovation Ltd., Loughborough Innovation Centre , Loughborough University Science and Enterprise Park (Holywell Park) , Loughborough , U.K.

[c] Photonics Research Group, Department of Electrical Engineering, Faculty of Engineering , University of Malaya , Kuala Lumpur , Malaysia

Accepted author version posted online: 15 Jul 2013.Published online: 29 Jul 2013.

To cite this article: K. F. Tamrin , Y. Nukman & S. S. Zakariyah (2013) Laser Lap Joining of Dissimilar Materials: A Review of Factors Affecting Joint Strength, Materials and Manufacturing Processes, 28:8, 857-871, DOI: 10.1080/10426914.2013.792413

To link to this article: http://dx.doi.org/10.1080/10426914.2013.792413

Materials and Manufacturing Processes, 28: 857–871, 2013

ISSN: 1042-6914 print/1532-2475 online
DOI: 10.1080/10426914.2013.792413

Taylor & Francis
Taylor & Francis Group

Laser Lap Joining of Dissimilar Materials: A Review of Factors Affecting Joint Strength

K. F. Tamrin[1,2], Y. Nukman[1], and S. S. Zakariyah[2,3]

[1]*Department of Mechanical Engineering, Faculty of Engineering, University of Malaya, Kuala Lumpur, Malaysia*
[2]*Advanced Technovation Ltd., Loughborough Innovation Centre, Loughborough University Science and Enterprise Park (Holywell Park), Loughborough, U.K.*
[3]*Photonics Research Group, Department of Electrical Engineering, Faculty of Engineering, University of Malaya, Kuala Lumpur, Malaysia*

Laser joining of dissimilar materials has been the subject of intensive studies in the past decade or thereabout. This is mainly due to the several benefits it offers when used to manufacture various electromechanical components for automotive, aerospace, electronics, and biomedical applications. There are many possible variations of joining dissimilar materials; this article, however, considers the main engineering materials in use today, namely, metal, polymer, ceramic, glass, and silicon. The strength of the joints determined by, inter alia, the material combinations, joining technique, and material treatment is crucial for the above mentioned applications if safety and reliability requirements are to be adhered to. Undoubtedly, the challenges posed by such complex selection of materials and process factors are unquantifiable and as such have been given a critical review in this article. The relationship between some important laser processing parameters and joint strength are also discussed. Furthermore, it has been observed that the joint strength can also be influenced by factors such as bubbles morphology, material preparation/treatment, depth of molten pool and formation of chemical bonds, and intermetallic phases and their effects are also reviewed and discussed. This article is concluded with an outlook providing the summary and key findings of the authors.

Keywords Dissimilar; Joining; Joint; Laser; Material; Strength; Welding.

Introduction

Joints between dissimilar metals have received great acceptance in power generation, petrochemical, nuclear, and electronics industries [1]. Combining metals and alloys of dissimilar properties have successfully removed certain constraints and rigidity in design while paving the way for technical and economic competitiveness over singularly-fabricated components [2, 3]. Similarly, it has been established that enormous benefits can be derived by combining materials of dissimilar classes such as metal/ceramic [4–7], metal/glass [8], metal/polymer [9–18], glass/silicon [19–22], glass/polymer [23], polymer/ceramic [24], among others.

Micro-electro-mechanical systems (MEMs) are generally fabricated on a silicon substrate due to the high adhesive property of the latter to a variety of materials [20]. Due to this outstanding mechanical strength, silicon-based microsystems are used for sensing and actuating purposes [19]. However, silicon has inferior resistivity to moisture [25] and is therefore generally replaced with polymer to overcome this problem. Meanwhile, thermoplastic polymers such as polyimide (PI) [9, 10, 14, 15, 17, 26], polyetheretherketone (PEEK) [27], polyethylene terephthalate (PET), [28–32], and parylene [25] show good resistance against some chemicals and thermal degradation. In particular, parylene has inert characteristics, which makes it a more suitable and useful material [25]. Thermoset polymers cannot be welded without additional intermediate layer; this is because their molecules cannot be reheated or re-formed [33]. Joints between dissimilar materials classes in MEMs and Bio-MEMs applications must fulfill tough requirements in terms of strength [23], thermal stress, fatigue, hermeticity [34], and long term stability [27, 35]. As a result, polymeric materials are usually combined with metals to fulfill the aforementioned test requirements. Commonly used metals for this application include titanium [9–18], kovar (nickel-cobalt ferrous alloy) [4, 36], platinum, gold, and stainless steel [28, 29]. Titanium and nitinol are some of the biocompatible metals being used for medical implants. Nitinol—also known as a "shape memory alloy" (SMA) because of its ability to "remember" and regain its original shape after undergoing deformation—is a suitable choice for applications in aerospace and medical sectors [27].

High demand for lightweight components to reduce cost, weight, and increase productivity has led to numerous designs of hybrid components and structures [37–40]. For example, carbon fiber composites have been widely used in aircraft and automotive constructions as they offer weight reduction while retaining good

Received November 3, 2012; Accepted March 4, 2013
Address correspondence to K. F. Tamrin, Department of Engineering Design and Manufacture, Faculty of Engineering, University of Malaya, 50603 Kuala Lumpur, Malaysia; E-mail: krolfikri@yahoo.co.uk

mechanical strength to weight ratio; this implies a reduction in fuel consumption. In comparison to metal, plastics are free from corrosion and are resistant to fatigue. However, monolithic composite materials do not conduct electricity. In airframe construction, materials with electrical conductivity property, such as metal matrix composites [41, 39], are considered crucial to ground electrical circuits as they dissipate lightning strikes and reduce electromagnetic compatibility (EMC) problems. Generally, metal and plastic complement each other to offer various positive features particularly in automotive and aerospace industries.

In addition, the high temperature stability, high strength, corrosion resistance, and wear resistance of ceramic [6] has made it a favored choice for some biomedical applications. For example, Al_2O_3, the most widely used bio-ceramic, is used in artificial joints and dental and middle ear implants [6]. Similarly, tetragonal zirconia polycrystal (TZP) ceramic is used for artificial fingers and dental implants [7]. Although glass is brittle in nature, it is however chemically durable and electrically insulating [19]. Biocompatible glass and silicon have been widely employed in implantable microsystems [25]. Typically, this type of glass is free of heavy metal, but it is "equipped" with compatible pH value, and it is electrolytically and hydrolytically stable [7].

There are several conventional techniques available to join dissimilar material classes offering one benefit or the other. For example, brazing is one of the established techniques for joining ceramic to metal, often employed to reduce the brittleness of the former. Nevertheless, the use of laser for similar purpose offers some additional advantages over conventional joining methods (as shown in Table 1). Although there are certain drawbacks using conventional joining techniques, a successful and optimum use of laser would require special considerations. This review describes the underlying principles of laser lap joining of dissimilar material classes in terms of material properties, experimental configurations, sample/surface preparations, and joint characteristics.

Principle of laser lap joining of dissimilar material classes

In general, laser lap joining is achieved by illuminating two pieces of clamped materials with a concentrated laser beam (Fig. 1). This process requires that one material is absorbent while the other functions as a transparent material. Laser beam is first transmitted through the transparent material; this induces heat at the material's interface which is sufficiently high to promote melting in that region. A joint is finally created when the materials are fused upon resolidification. In some instances, the generated heat is just enough to melt the material with a lower melting temperature [23, 30, 31]. Provided that the induced heat is sufficient to cause one of the materials to melt, the joining process will take place upon solidification. For this arrangement, a metal or plastic can be used as the base plate. Wild et al. [19] observed that employing polytetrafluoroethylene (PTFE) material as

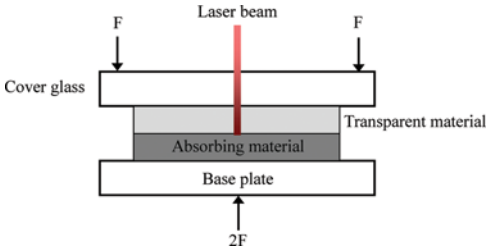

Figure 1.—A typical laser transmission lap joining arrangement of two materials using a laser beam. The laser beam is scanned across the material to create interfacial joint between two dissimilar materials (color figure available online).

Table 1.—Qualitative advantages of laser lap joining of dissimilar materials classes over conventional techniques.

Joint configuration	Application	Example of conventional technique	Common drawback of conventional technique in comparison with laser joining
Glass-silicon	Microsystems and microsensors	Anodic bonding	High temperature process, long process time [19], and high electric field 1,000–2,000 V [49]
Metal-glass	Hermetic encapsulation in electronics and electrical components	Glass frit	Frit curing in a furnace detrimental to heat-sensitive components and miniature components [36]
Metal-polymer	i) Lightweight automotive and aerospace structures, and ii) Microsystems and microsensors	i) Injection molding, and ii) Adhesive	i) Mould to be made with tight tolerances but only applicable to a specific purpose, and complexity in part handling [40] ii) Inferior long-term stability, adhesive shrinkage, and biocompatibility issues [23]
Metal-ceramic	i) Automotive and aerospace parts, and ii) Electrical and electronics packaging	i) Fusion welding, and ii) Ultrasonic welding	i) Large heat affected zone [47] and poor optical quality especially for automotive parts ii) Ultrasonic vibration can damage electrical components [33]
Ceramic-polymer	Lightweight automotive and aerospace structures	Mechanical fastening	Design inflexibility and low production rate [37]

a base plate instead of aluminium would cause a 30% reduction in the minimum laser power required for initial bond-breaking. This is due to the efficient thermal insulating property of PTFE having a thermal conductivity three order of magnitude less than that of aluminum [19]. Laser transmission joining can also be performed even when both materials are not transparent, for example, joining of metal with ceramic [4].

The effect of materials properties on laser joining

The effectiveness of laser welding depends greatly on the physical, thermal, optical, and chemical properties of the materials to be welded, and this is discussed in this section.

Effect of Thermal Expansion

Laser joining of two dissimilar materials especially when there exists a large difference in thermal expansion is challenging, as it results in high residual thermomechanical stresses in both materials when cooled [42]. At high cooling rates, thin materials of less than 0.5 mm are susceptible to cracking [39], while non-uniform heating of ceramic resulted in fracture [4]. It should be noted that, in some instances, high cooling rates are deemed beneficial to avoid excessive polymer degradation [39]. Mian et al. [23] have shown that, unlike with a lower power density diode laser, high power density fiber laser can prevent cracking during laser welding of dissimilar materials. Gower et al. [39] also observed that at high cooling rates of metal/polymer joint, cracking can be prevented by using pulse shaping.

A sudden change in thermal expansion initiating cracking in ceramic and glass joint was also reported [7]. Due to this reason, glass is usually coated with titanium using an established coating process before being joined with polymer [9, 15, 7, 26, 23], since an intense laser heat source could initiate cracking in glass. Interestingly, without the metal coating process, Ozeki et al. [8] reported a successful direct joining of copper (Cu) with the non-alkali glass using both femtosecond and nanosecond lasers, though there exists large thermal expansion difference of about 77%. Glass and silicon joints can be generally found in MEMs devices because they do not differ much in thermal expansion coefficients [20, 43, 44]. For instance, Pyrex glass and a polished single crystal silicon [19] differ by about 5%. Recent results and trends in ultrashort laser welding and joining glass-glass and glass-silicon are available in [45].

On the other hand, laser joining of borosilicate glass and fused silica, with large difference in their thermal expansion coefficients, required a considerably huge applied clamping pressure of 40 MPa to ensure that the gap is less than $\lambda/4$ [46]. This extremely small gap is essential to avoid ablation from occurring at these two surfaces. This was found to be the main cause of a reported, unsuccessful joining process [42] at the expense of unwanted stress concentrations [47]. Nonetheless, the value was 40 times greater than that employed in a successful joining of PET/Ti joint [18]. The clamping pressure required for joining fluorinated ethylene propylene (TeflonFEP) with Ti was even less at 0.414 MPa [9, 12].

Laser Absorptivity as a Function of Surface Roughness

Removing the oxide layer from a material surface is important to ensure a reliable joint strength [28], though this is not always the case. For example, comparison of joint performance between PET/PO-Cu (PO stands for pre-oxidized layer) and PET/Cu (without pre-oxidized layer) using a Nd:YAG laser revealed that the former shows 40% greater tensile shear load strength [31]. Since polished Cu has a relatively high thermal conductivity and reflectivity (Table 2), the oxide layer deposit is reckoned to increase the surface roughness which indirectly increases a material's absorptivity. This subsequently facilitates heat transfer across the interface. Secondly, higher bond strength can be attributed to an increase in joint area [30, 31] as a result of the high heat requirement for the initial melting of the oxide layer. These two factors enhanced the joint strength of the PET/PO-Cu joint.

In the case of PET/Cu joint, the bond strength was solely fostered by the bubbles formation at the interface [48] while Cu remained solid irrespective of the heat input [30, 31]. This concurred well with the numerical analysis which showed a rapid distribution of heat throughout the Cu material [30]. Significantly, the reflectivity of most metals reduces and their absorbent tendency becomes higher at wavelengths below 900 nm [49]. This suggests that Nd:YAG laser ($\lambda = 1{,}064$ nm) is unsuitable for joining Cu material. However, to circumvent this, O_2 gas can be used as an assist gas to increase the absorptivity of Cu under CO_2 and Nd:YAG laser welding [31]. Meanwhile, the bond strength of silicon/glass joint strictly depends on silicon absorption coefficient and its thermal conductivity to laser parameters. Wild et al. [19] observed that non-optimum laser processing parameters resulted in an unwanted crack, and unstable bonding and surface melting of the silicon. The high absorption coefficient and low thermal conductivity of a silicon material also results in minimal heat affected zone (HAZ), allowing low temperature around the entire silicon wafer. This positive feature proved to be useful in packaging or fabricating temperature-sensitive items [34].

Effect of Glass Transition Temperature

The use of laser in joining metal and polymer has the advantage of controlling polymer degradation which

Table 2.—Normal, spectral absorptivity of Cu at important wavelengths [79].

Wavelength / material	300–600 nm	1.06 μm	10.6 μm
Copper (polished)	0.05	0.04	0.01–0.03
Copper (rough)	0.05	0.1–0.3	0.05–0.10
Copper (oxidized)	0.85	0.5	–

cannot be obtained by using micro-soldering or brazing. For instance, PET is likely to degrade in soldering technique because it has lower glass transition temperature (T_g) than that of soldering temperature [31]. Miyashita et al. [50] studied the weldability of PET ($T_{g,PET} = 80°C$) and PC ($T_{g,PC} = 140°C$) with stainless steel (SUS304), the maximum shear tensile strengths of SUS304/PET. and SUS304/PC joints were measured as 6.5 MPa and 2.1 MPa, respectively. This difference in strength can be attributed to the difference in glass transition temperature of the polymers [50], where PET melts faster in comparison to PC at the same energy density. As a result, SUS304/PET joint has larger bonding area with sufficient optimum bubbles formation, thus promoting higher bond strength [50].

Effect of Young's Modulus

In laser transmission joining, laser is usually focused at the interface. Hence, an "intimate" contact (firm clamping of two surfaces with minimum gap in between them) is necessary to avoid unwanted stray laser beam and reflection off the interface as this would increase the HAZ. This is also required to ensure efficient thermal conduction across the materials. Although "intimate" contact is desirable for successful joining, the difference in Young's modulus between dissimilar materials may promote stress concentrations at the interfacial region [47]. In particular, ceramic-to-metal joint has non-uniform, complex stresses distribution along the interface as well as within the ceramic [47]. To overcome these stresses, a filler metal is normally introduced and placed between the samples [5, 7].

Processing parameters

Laser-Matter Interaction and the Resulting Joint Strength

The characteristic of laser beam used to process the materials is crucial to the strength of the joints. Laser material interactions are well documented in the literature [51–56]. For this application, the key features of interest are the energy density, laser type/wavelength, and operation mode. Selection of suitable laser power and welding speed are fundamental in ensuring optimum joint strength. These two parameters are however inseparable; in other words, they depend on each other. Mian et al. [23] investigated the strength performances of glass and PI that were joined using two different types of lasers. The optimum laser parameters used in the experiments can be found in Table 3. The power and beam spot diameter of diode laser used for the study were greater than that of Yb-doped laser, but the latter produced power density that was more than six times the former. This over 16% increase in power density resulted in strengthening the joining bond between the materials. In other words, a high power density fiber laser produced better joints than diode laser with a lower power density.

Table 3.—Bond strength of the glass/Pi samples processed with diode and fiber lasers [23].

Laser used	Wavelength (nm)	Power (W)	Spot diameter (mm)	Power density (W/mm^2)	Average bond strength (N/mm)
Diode laser	800	3	0.8	5.97	6.19
Fiber laser	1,100	1	0.2	31.83	7.34

Often, large width bond is desirable for strong bond strength [30]. In contrast, small laser spot diameter is preferred to ensure that the heat distribution around the sensitive area is well controlled, especially in heat sensitive packaging. It was shown [57] that for joining glass to silicon, an Nd:YAG laser produced a narrower bond joint, which was said to be eight times less than that of the diode laser, due to its improved focusability in comparison to the latter. However, no comparative verification of the shear strength was carried out for these two competing laser machines. In addition to the use of pulsed lasers for glass-silicon bonding [43, 58], successful joining was reported using continuous wave (CW) lasers [44, 20] provided that the laser wavelength can be efficiently transmitted through the transparent glass. This, however, precludes the use of a CO_2 laser ($\lambda = 10.6\,\mu m$) for a glass since the latter exhibits high absorptivity coefficient at this wavelength. Similarly, titanium and kovar absorb very well at this wavelength range [4].

A pulsed laser is favored over a CW laser due to short thermal cycle [8, 39]. It has been shown [39] that pulse shaping can limit the weld crack length of an aluminium-polypropylene laminate joint; this is achieved by using a top-hat beam profile to ensure homogenous beam distribution across the interface as the laser process progresses. This type of beam profile minimized vaporization of the polypropylene material [39] through controlled thermal decomposition of the polymer. This result only relates the weld penetration between the two substrates to reduced bond strength. Unfortunately, some porosity and undercut were observed when the joint was performed at high laser power [39]. Similarly, the polymer decomposition became more rapid due to oxidation [39]; this can be mitigated by using an inert argon gas [7, 39] or nitrogen gas to cool down the plastic surface [28].

Besides, ultrashort lasers have been shown to be desirable for joining materials with large difference in thermal expansions [42, 8, 59] and highly reflective materials [31, 8]. Ozeki et al. [8] reported that when a femtosecond laser was used to irradiate the interface, a filament-type beam was formed across the two materials with spot diameters varying within few microns along the optical axis [42, 59]. In joining dissimilar glasses, the ellipsoidal filament was measured to be 30 μm long [42] which simultaneously melted down both materials due to non-linear field ionization [60, 61]. The heat generated within the focal volume also facilitated the formation of electron-ion plasma which induced localized melting and quenching of both materials [60, 61]. Although there exist various established techniques to join metal with glass, Ozeki's work seems to be the only publicly

TABLE 4.—An example of a successful experiment in laser lap joining of metal to glass.

Combination of metal and glass	Thickness (mm)	Optimum laser parameters	Specific processing step	Bond strength	Comment	Ref.
i) Copper, $\alpha_{Cu} = 17.0 \times 10^{-6}/°C$ ii) Non-alkali glass, $\alpha_{Gl} = 3.9 \times 10^{-6}/°C$	i) 1.0 ii) 0.7	fs-laser:$\lambda = 800$ nm; $p_d = 130$ fs; f = 1 kHz; E = 0.4 μJ/pulse ns-laser:$\lambda = 527$ nm; $p_d = 600$ ns; f = 1 kHz; E = 50 μJ/pulse	40 MPa clamping pressure	fs-laser > 16 MPa; ns-laser > 13 MPa	Joint was free from crack and void.	[8]

E = energy, f = frequency, α = thermal expansion coefficient, P = power, P_p = peak power, P_R = ramp up power, P_d = power density, d_s = spot diameter, t = duration, p_d = pulse length.

available literature within the scope of laser lap joining of metal and glass as far as the authors are aware. As a comparison, the maximum Cu-glass joint strengths welded using nanosecond (ns) and femtosecond (fs) lasers and their respective laser parameters are compiled in Table 4. While the pulse energy of ns-laser was two orders of magnitude greater than that of fs-laser, the copper substrate did not melt in the former case because there was no filamentation formed within [8]. This can be attributed to poor thermal conduction across the interface as a result of low energy density (Fig. 2). In addition, the HAZ produced by fs-laser was found to be smaller than that of ns-laser [8].

It should be noted that the use of statistical analysis and mathematical modeling are useful in dealing with numerous process parameters (laser power, scanning speed, pulse repetition rate, stand-off distance, seam width, and joint quality) [29, 49]. An example of a widely used optimization technique is a response surface methodology (RSM) which establishes relationships between the input and output variables [29].

The position of the focal point on the workpiece has significant influence on joint strength. It is usually varied as a means to decrease the power density at a constant power input. Power density, P_d is governed by

$$P_d = \frac{4P}{\pi d_s^2}, \quad (1)$$

where P is the beam power and d_s is the beam diameter. Wang et al. [18] varied the position of focus from 800 μm to 900 μm spot diameter to prevent excessive overheating and avoid unnecessary burning of polymer.

The Role of Welding Speed and Power/Energy

Formation of sufficiently strong joint strength requires the selection of optimum power/energy density and scanning speed parameters. It is observed [14] that a strong bond could be obtained when the joint was made at low speed and medium power. The joint strength was influenced by adequate melting and wetting of polymer to the surface of metal [38]. In particular, PI has high surface tension in comparison to other plastics which promote strong intermolecular forces to the metal [62]. However, excessive heat generation at low scanning speed might initiate undesirable overheating and burning of plastic material [38, 18], polymer degradation, and high pore formation [38]. Meanwhile, at high speed and high power, the unexpected weak bond strength [14, 18] can be attributed to an inefficient laser-matter interaction. In this case, the laser had less contact time to induce sufficient thermal conduction and melting at the interfacial region. For instance, the effect of power on porosity is more pronounced than the effect of joining speed on bonding strength for joining polyethylene terephthalate glycol (PETG) film with stainless steel (SUS304) sheet [38].

Typically, strong bond joint is achieved at moderate power and moderate welding speed [18, 38]. Figure 3 illustrates the effect of laser power on bond strength at various welding speed. For example, as high as 90 MPa joint strength of PET/Ti joint can be achieved

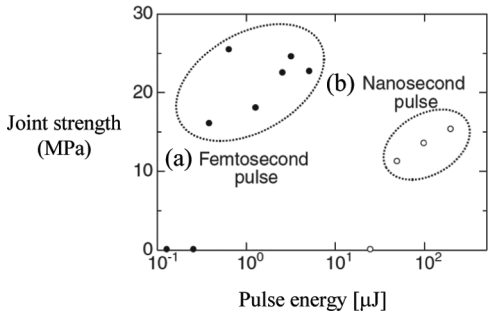

FIGURE 2.—Effect of irradiated pulse energy on joint strength for Cu/glass materials using: (a) femtosecond pulses and (b) nanosecond pulses [8].

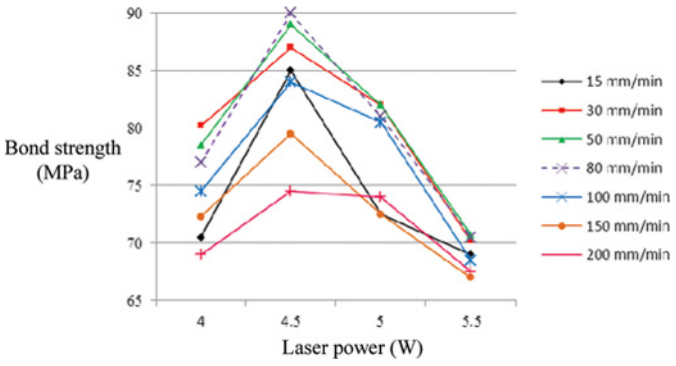

FIGURE 3.—Bond strength measurement of Ti/PET joints due to changing in laser power and scanning speed [18] (color figure available online).

at moderate welding speed and power of 80 mm/min and 4.5 W, respectively [18]. However, Tan and Tay [49] observed that for joining silicon to quartz, high laser power and low scanning speed were needed. This is because the authors used an intermediate layer which requires an additional power density for that layer to melt at the initial stage.

Variants of Laser Lap Joining of Dissimilar Materials

A novel technique known as LIFTEC (Laser-Induced Fusion Technology) was developed to create much stronger joint between metal and polymer, or ceramic and polymer components [40] particularly useful for automotive parts assembly. Based on laser transmission welding, a laser is transmitted through a block of transparent base plastic to heat up a fastener made of metal or ceramic. As a result of localized heat at the interface, the base is melted down. At this juncture, the fastener is mechanically pushed inside the plasticized base and finally forms a permanent joint upon cooling. In separate validation studies, the mechanical strength of a grooved metal bolt joined to the plastic base was found to be about 7% greater than the conventional screw joint [40], as shown in Fig. 4. Readers are referred to the review in [63], which comprehensively described joining methods of polymers and polymer-metal hybrid structures, but the review did not cover laser joining of plastic with metal.

Glass is typically bonded to silicon using a state-of-the-art anodic bonding technique. In comparison to laser illumination, anodic bonding involves both thermal (400°C) and electrical (up to 2 kV) processes [49]. In this state, sodium, lithium, or aluminium ions from the glass are diffused into the silicon since glass has longer melting duration compared to silicon [58], which subsequently forms a solid chemical bond [64]. The applied electric field also causes oxygen gas to be released from the glass [64]. Meanwhile, laser transmission joining of glass to silicon can be accomplished in various processing conditions as noted in Table 5. In joining glass to silicon, formation of a molten pool [43, 58] is not necessarily the main requirement since the bond strength is influenced by ions diffusion from glass to silicon. Hence, it is possible to join them below their glass transition temperatures as demonstrated in [19, 20], which reduces heat input and HAZ. Nonetheless, Mescheder et al. [44] demonstrated that at low energy density, a combination of fusion bonding and eutectic bonding had produced considerably high bond strength comparable to bond strength of an anodic bonding. Some advantages of laser illumination over anodic bonding as noted in [19] are the following ones:

1. Selective laser bonding means small HAZ;
2. Small bonding geometry; and
3. Release of gases is eliminated since there is no supply of an electric field.

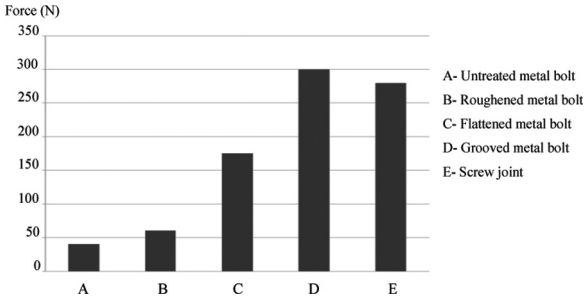

FIGURE 4.—Mechanical strength of different geometries of metal/plastic joints [40].

SAMPLE PREPARATION

Cleaning

Sample preparation is important since the sample surface can influence energy absorption of the incident laser beam [65] and bond integrity. Glass and polymer samples are normally cleaned from dirt and contaminants using alcohol solutions, e.g., methanol [29, 31, 51, 58, 66] in an ultrasonic bath [31, 29] and subsequently rinsed with deionized water [58]. In addition to ultrasonic cleaning, silicon material is wet-cleaned using hydrogen-peroxide-based solution [49]. On the other hand, metals and their alloys are generally cleaned using an acetone solution [18] in an ultrasonic bath [38]. For instance, a metallographic sand paper was used to grind the metal surface [18, 31] that was contaminated with the preexisting oxide layer [31]. Flowing nitrogen gas was subsequently used to dry the samples because of its inert and volatile properties [49, 19, 58].

Interestingly, Wang et al. [18] reported an unusual cleaning of PET sample using an acetone solution in an ultrasonic bath and then dried using a hot gas. Polymer decomposition or swelling might have occurred as a result of chemical interaction with the acetone. This kind of surface degradation or unintentional surface restructuring could be the factor that fostered strong bond strength of PET/Ti joint of 90 MPa. In addition, the authors [18] used a drying oven for a period of 12 hours to remove moisture and dust on titanium surface [18].

On the contrary, Lubna et al. [67] proposed a new method of cleaning the sample utilizing sequential combinations of Alconox solution (degreasing soap solution), distilled water, acetone, and methanol. The joints strength was measured as 29 MPa and 13 MPa for the new and regular methods respectively. X-ray photoelectron spectroscopy (XPS) results indicated that an ordinary cleaning of the sample surface had poor adhesion between surfaces due to considerable amount of adhered carbon contaminants [67].

In joining Mg to PET, Wahba et al. [28] reported that removal of an oxide layer on thixomolded Mg alloy surface by grinding, resulted in reduction of laser power by 300 W from the actual power of 1,000 W. The higher input energy was probably required to first heat up the oxide layer before the laser could penetrate to the base material. The oxide film could have originated from

TABLE 5.—Examples of some successful experiments in laser lap joining of glass to silicon.

Combination of glass and silicon	Thickness (mm)	Optimum laser parameters	Specific processing step	Bond strength	Comment	Ref.
i) Pyrex glass, $\alpha_{Py} = 3.25 \times 10^{-6}/°C$ ii) Polished single crystal silicon, $\alpha_{Si} = 3.43 \times 10^{-6}/°C$	i) 0.50 ii) 0.55	$\lambda = 1{,}064$ nm; $d_s = 300$ μm; $15 < P < 30$ W; $100 < v < 400$ mm/min	Clamping pressure = 10–30 MPa	–	No quantitative evaluation of bond strength. Stable bonding with no formation of molten pool, crack, or melting of silicon while both materials remained solid. Bond was formed due to ions diffusion.	[19]
i) Pyrex glass ii) Polished single crystal silicon	i) 0.50 ii) 0.50	$\lambda = 355$ nm; $d_s = 1$ mm; $8 < E < 22$ mJ; $4 < p_d < 6$ ns;	Indium intermediate layer (4 μm thick)	2.6 MPa	Although the bond was formed by conduction welding, the surface of liquid pool was found to remain unbroken. Bond strength was comparable to the yielding strength of indium of 2.6 MPa [43].	[43]
i) Pyrex glass ii) Standard silicon wafer	Standard thickness	$\lambda = 1{,}064$ nm; $d_s = 100$ μm; $P = 38$ W; $v = 20$ mm/min	Al intermediate layer (100 nm thick), eutectic conc. in Si = 11.3%, eutectic temp. = 577°C	44.0 MPa	Intermediate layer formed a eutectic alloy with silicon resulting in bond strength comparable to that of anodic bonding.	[44]
i) Pyrex glass ii) Polished silicon wafer, surface roughness <2 nm	i) 0.50 ii) 0.50	$\lambda = 1{,}064$ nm; $d_s = 800$ μm; $E = 65$ mJ; $p_d = 12$ ns;	No intermediate layer	–	No quantitative evaluation of bond strength. Direct laser joining where bond was created due to Al and Na ions diffusion to silicon. Both materials melted but silicon solidified faster than glass due to longer melting duration of glass.	[58]
i) Glass ii) Standard silicon wafer		$\lambda = 810$ nm; $d_s = 3 \times 8.5$ mm; $P_d = 1$ W/mm^2; Curing temp. = 300°C	9.4 μm thick benzocyclobutene (BCB) as an intermediate bonding layer	Shear force 200 N	BCB bonding layer was cured <2 s when compared to oven curing of few minutes. Curing occurred at temperature well below the glass transition temperature of silicon and glass.	[20]

TABLE 6.—Optimum sample preparation method for various materials.

Material	Optimum sample preparation method
Metal	Metals and their alloys are cleaned using an acetone solution in an ultrasonic bath.
Glass	Glass is cleaned using alcohol solutions such as methanol in an ultrasonic bath and subsequently rinsed with deionized water.
Polymer	Polymer is cleaned using alcohol solutions such as methanol in an ultrasonic bath and subsequently rinsed with deionized water.
Silicon	Silicon is cleaned using acetone solutions (10 min), rinsed with deionized water (5 min), cleaned again in isopropyl alcohol (10 min) and finally rinsed with deionized water (5 min). All procedures are done in an ultrasonic bath at 35°C [49].
Ceramic	Ceramic is cleaned using isopropanol or acetone solutions such as methanol in an ultrasonic bath and subsequently rinsed with deionized water.

the thixomolding process since Mg has high affinity for oxygen. At optimum laser processing, the joint strength for grinded and received specimens were 1,500 N and 900 N, respectively [28]. The oxide layer generally becomes porous and loose at high temperatures [68], and this may account for porosity and gas entrapment during laser welding. These inherent defects further degrade the mechanical strength.

Table 6 provides optimum surface preparation methods of various materials prior to joining.

Metal Surface Restructuring

To address the materials' incompatibility in joining plastic and metal, Roesner et al. [62] initiated pretreating of a metal surface via laser structuring. A 40 W μs-pulsed Nd:YAG laser was used to form a groove pattern on a 2 mm thick stainless steel surface as schematically shown in Fig. 5. The process was repeated three times to achieve an undercut structure (40 μm width, 50 μm depth). As a result of sufficient clamping pressure between plastic and metal, the molten plastic in the interface was forced to flow inside the grooves and subsequently solidified to form micromechanical interlocks. The strength of the resultant interlocks depends on the number of grooves and their widths and spacing between them. In this regard, a term referred to as structure density (SD) was proposed to quantify the interlocks. SD is defined as the width of the structure divided by the distance between each structure. It was found that $SD > 0.7$ is a suitable value for producing high mechanical shear strength [62].

Wahba et al. [28] showed that an increase of 15% in joint strength was achieved when Mg alloy surface was melted prior to laser welding, producing pores near the surface and adding to the pre-existing pores in typical Mg alloy surface. Non-uniform microstructures will be created when the porosity on the surface is subjected to grounding. The increase of joint strength was the result of a mechanical anchor effect due to solidification of plastic fluid inside the pores.

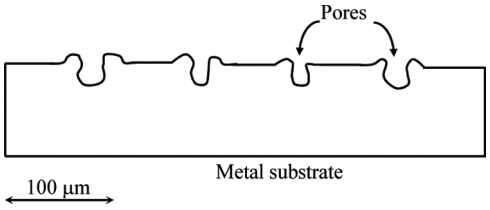

FIGURE 5.—Cross-sectional view of a microstructured stainless steel after metal surface restructuring using a laser source. When firmly clamped, melted plastic is forced to flow into the microstructures [62].

In addition, Kawahito et al. [69] demonstrated the use of 807 nm diode laser in pre-processing step to minimize the thickness variation between a metallic glass sheet $Zr_{55}Al_{10}Ni_5Cu_{30}$ and a PET film. The laser power density was adjusted to $5\,W/mm^2$ which is barely enough to melt the metallic glass, resulting in virtual removal of air gaps and creation of a temporary joint [69].

Anodization

Yusof et al. [32] studied the effect of anodizing 1 mm aluminium alloy (A5052) surface prior to joining with 0.5 mm PET film. For this study [34], an A5052 specimen was first subjected to typical ultrasonic surface cleaning using an acetone solution and followed by immersing it into an electrolytic bath containing sulphuric acid for 30 minutes at 23°C and 12 V. After rinsing with distilled water, the specimen was dipped into a chemical solution to seal the pores, resulting in the formation of 10 μm thick anodizing layer [32]. The joint was formed using pulsed Nd:YAG laser regulated at 55.8 J and 20 ms. The shear strength of the anodized PET/A5052 joint was found to increase by 36% when compared to a similar joint that has not undergone any treatment.

Meanwhile, surface treatment by anodizing prior to welding was observed to improve the strength of PET/A5052 joint by 50% at minimum pulse duration, compared to "as-received" joint [32]. As a result of anodizing, the reflectivity coefficient was found to have decreased due to alteration of metal crystallography. This allows much input heat energy to be absorbed at the interface, producing broader joint area and greater bond strength. In a separate study, PET/SUS304 joint produced relatively higher shear strength compared to PET/A5052 joint by an approximately 1.4 times at optimum laser processing parameters [30].

Surface Activated Pre-Bonding

An appropriate clamping pressure/force is generally required for sound and reliable joining [9]. When two materials are firmly clamped, the focusing of laser at the interface can be easily and accurately achieved. Since glass is naturally brittle, the applied pressure may cause bending or unwanted crack, which might further

complicate the joining process. Therefore, Shi et al. [21] suggested a surface activated pre-bonding technique in joining 525 μm Pyrex glass wafer to 380 μm polished single crystal silicon. Both the glass and silicon were subjected to normal cleaning procedure, and the surfaces were further chemically activated as described in [70]. This resulted in intimate bonding between the two surfaces as they both became hydrophilic. Hence, the technique eliminates the need for clamping force while preventing any residual stress due to bending and cracking. After laser bonding, the shear strength of the joint was measured within the range of 6.3–6.8 MPa.

Effect of an Intermediate Layer on Joint Strength

To obtain a strong joint in lap joining arrangement, another crucial factor is the flatness or/and smoothness of materials' surfaces. Often this is difficult to realize; however, sufficient clamping pressure has been applied to reduce surface roughness of differing materials. Therefore, the surface characteristic of materials is usually quantified and represented by surface roughness. The surface roughness or simply roughness is a measure of a local microscopic characteristic of a surface usually denoted by a capital letter R following a letter subscript to indicate the type of roughness. The root mean square average, R_q [71] obtained using the equation below is one of the commonly used type of roughness in conjunction with Ra, the arithmetic average roughness, where n is the sample number, and y_i represents the distance from the center line:

$$R_q = \sqrt{\sum_{i=1}^{n} \frac{y_i^2}{n}}. \quad (2)$$

Therefore, in order to circumvent the above mentioned problem, i.e., roughness, an intermediate layer is usually introduced. In addition, the large difference in thermal expansion between materials can be overcome by using a layer with an intermediate thermal expansion coefficient. Application of Al or Au as an intermediate layer to bond silicon and Pyrex 7740 (boron silicate glass) was shown to offer joint strength that is comparable to anodic bonding [44]. The average measured strengths for both (Al and Au) were greater than 40 MPa. This strength is attributed to the formation of eutectic bonding, and they are further strengthened by successful laser joining process. It should also be mentioned that Au intermediate layer produced an average bond strength about 1.6 times higher than that of Al layer because of lower eutectic temperature of Au/Si and high diffusivity of Au in Si [44]. Sufficient joint strength was also achieved using a polymer as an intermediate layer to laser-bond glass and silicon [20]. Other materials used as an intermediate layer for joining dissimilar materials classes include: indium [43], silver [7], carbon black [72], and thermosetting polymer benzocyclobutene (BCB) [22] for the glass/silicon bonding and a mixture of Sn and Au for the silicon/quartz bonding [49]. In particular, carbon black is deposited to absorbing materials to increase the absorptivity and hence the penetration depth [72]. In comparison to other intermediary layers, Au produced the most excellent bond strength in the region of 20–90 MPa [44]. This said, glass and silicon can, however, be directly joined without an intermediary layer, as demonstrated in [57, 73].

Similarly, there are reports on studies being carried out on joining titanium-coated glass with polymer since the former possesses good biocompatibility property [23, 7, 15, 26, 10, 35, 74]. Initial studies of laser bonding of titanium-coated glass with polymeric film showed that titanium coating film, with less than 50 nm thickness, would produce poor bond strength while reliable bond strength was achieved when the thickness is in the range of 50–200 nm [75]. Results of the study on the effect of coating thickness on shear strength indicate that, as coating thickness increases to 400 nm, the surface roughness also increases [74]. This feature is positive and favorable as it enhances mechanical interlocking between PI and Ti-coated glass. In fact, the existence of Ti-C-, Ti-O-, TiO_2-type chemical bonds is believed to offer strong bond strength in the range of 50–400 nm thickness [74]. These bonds (carbon and oxygen bonds with titanium) are obtained from the carbonyl group ($>C=O$); the latter originate from PI molecular chains [9].

One outstanding intermediate layer that can be used to join two dissimilar materials is glass frit. Glass frit is typically used for hermetic sealing in miniature devices before heated in a furnace. Wu et al. [36] demonstrated that when glass frit paste is combined with localized laser source, the need for furnace is removed; this allows materials with much varied chemical and physical properties to be easily joined. A successful joint was demonstrated using this method to join kovar to leadless co-fired ceramic (LCC), aluminium nitride (AlN), low temperature co-fired ceramic (LTCC), and silicon [36]. Since curing of glass frit paste requires bonding temperatures in the region of a few hundred degrees Celsius [76], this would reduce the demand for laser energy/power and hence the cost. However, the method requires minimum pressure to ensure sound mating between two surfaces [36].

Joint characteristics

Laser Assisted Metal and Plastic (LAMP) and Bubble Formation

Katayama and Kawahito [48] were first to realize that a stable metallic or covalent bonds can be formed between metal and plastic. The authors introduced a technique that is simply based on laser transmission joining and known as Laser Assisted Metal and Plastic (LAMP). In this technique, the laser beam is initially transmitted through the plastic which causes a sufficiently high temperature rise in the interfacial region of the metal and plastic. The plastic is partly melted or decomposed at the interfacial region due to thermal conduction of the heated metal, which has been facilitated by the applied clamping force. At this state of high

TABLE 7.—Bond strength of the samples processed with LAMP technique.

Joint configuration	Power (W)	Scanning speed (mm/s)	Bond strength (kN)	Ref.
PET/SUS304	500	6	3.0	[48]
PET/Si_3N_4	170	4	3.1	[24]

temperature, bubbles are formed from the melted plastic which then undergo expansion according to input heat energy. Finally, physical or chemical bonding between them is achieved [48].

A direct laser bonding of 2 mm thick PET with 3 mm thick SUS304 was found to produce a shear load of 3.0 kN. Such high bond strength in LAMP joining was the result of the physical and chemical interactions characterized by the formation of gas bubbles, having suitable sizes and quantity, within the melted region of the plastic near the joint [28, 48]. Similarly, LAMP technique [48] was shown to be employed for bonding Si_3N_4 ceramic to PET without any intermediary pre-processing step [24]. In addition to bubbles formation, transmission electron microscope (TEM) observation revealed that the joint was firmly bonded on atomic or molecular level through an anchor effect. This is as a result of the liquid plastic flowing into the nanoscale ceramic hollows and subsequently solidified [24]. Hence, this mechanical interaction (anchor effect) may account for the slight increase in tensile shear strength of ceramic/PET joint [24] as shown in Table 7.

Recently, Wahba et al. [28] utilized the LAMP technique to compare two lap joint configurations, namely, PET resides at the top of AZ91D thixomolded Mg alloy and vice versa. Surprisingly, the joint strength produced using the second configuration is two-third higher than that of the conventional configuration. The recorded higher strength joint in the second setup is most likely due to discrete bubble formation near the interface as illustrated in Fig. 6. This is because discrete bubbles allow greater joint area to be achieved between dissimilar materials and hence higher bond strength. Meanwhile, lower bond strength is due to fractures initiated across the bubble structure and the ''networked morphology'' could only allow smaller joint area. At low scanning speed, the bubble size gets larger and the quantity increases because of the relatively high input heat. Unfortunately, this causes interface fracture that occurs across the bubble structure [28]. Tillman et al. [38] observed that a high quantity of bubbles leads to weak joint strength and vice versa; this is in agreement with the findings in [38, 50].

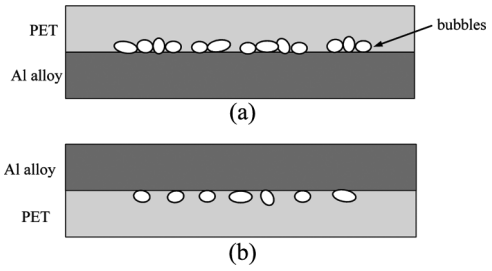

FIGURE 6.—Illustrations of (a) networked bubbles and (b) individual bubbles morphology. The latter exhibits higher bond strength since it has lower bubble quantity, hence allowing greater joint area. Meanwhile, lower bond strength of the former is due to fracture introduced across the networked bubbles and lesser joint area between the two materials.

Joint Strength as a Function of Molten Pool Depth

While investigating the effects of molten depth on joint strengths of PET/A5052 and PET/SUS304 using a Nd:YAG laser spot welding, Yusof et al. [30] observed the joint strength to be proportional to the molten pool depth [30]; in other words, increase (or decrease) in joint strength results in a corresponding increase (or decrease) in molten pool depth. The molten pool depth of PET/SUS304 was shallower (20 μm depth) with a larger area (570 μm width), when compared to PET/A5052 that had the feature of a keyhole welding. The keyhole depth was measured to be $\frac{1}{4}$ (250 μm) of the A5052 thickness. Interestingly, the tensile shear load of the PET/SUS304 joint was found to be approximately two times greater than that of PET/A5052 [30], probably due to the bubbles formation around the interfacial region [48]. This points to the fact that the combined characteristics of bubble formation and greater joint area outweigh the benefits offered by the keyhole feature. In addition, the input heat requirement of SUS304 was about two times lower than that of the A5052 [30] due to the differences in their material reflectivity and conductivity coefficients. It should be noted, however, that the bond strength of glass-silicon does not depend on the formation of a molten pool because, the laser joining process occurs below their melting temperature [19]. Instead, the strength is attributed to solid chemical bond due to ion diffusion from glass to silicon.

Formation of Chemical Bonds

Formation of chemical bonds within the joint microstructure also contributes to the overall joint strengths. Pi/Ti and Pi/TiG (TiG stands for titanium-coated glass) joints have been extensively studied by research groups in Wayne State University and Fraunhofer USA [10, 15, 23, 35, 67]. For instance, Newaz et al. [15] observed that the bond strength of Pi/TiG is approximately 1.5 times higher than that of Pi/Ti. The failure in Pi/Ti joint was noted to occur within the polyimide, while for Pi/TiG, in the glass substrate [15]. This implies that, in both cases, polyimide was strongly bonded to the titanium surface as a result of the formation of strong Ti-O and Ti-C chemical bonds [15, 18]. The induced bond strength seems to be comparable to bond strength of glass-Ti joint that was produced by metal-coating process. It should be stated that the measurement of bond strength in Pi/TiG was affected by flexural failure introduced by the test machine and the subsequent stress propagation to the vicinity of the joint [14, 15].

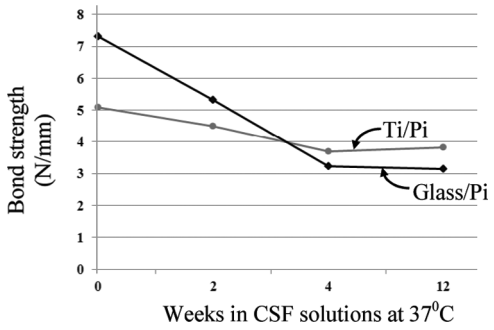

FIGURE 7.—A graph showing the relationship between the bond strengths of titanium/polyimide and glass/polyimide microjoints and CSF exposure time [15].

On the contrary, when these joints were dowsed in an artificial cerebrospinal fluid (CSF) for 28 days, Pi/Ti joint appeared to be 1.2 times stronger than that of Pi/TiG and the measured strength reductions are 25% and 57%, respectively (Fig. 7). According to [77], polyimide has high water uptake (1% on average) and high water transmission rate (1.350 g mm/m^2 day). This suggests that water absorption through the polyimide could promote oxidation at the interfacial region [15]. Since Ti-O bonds are not generally stable, they are oxidized to form a stable TiO_2, which accounts for slight stronger bond in Pi/Ti joint.

In comparison, TeflonFEP has an average water uptake of <0.01% and water transmission rate of 0.178 g mm/m^{2}day [77]. Joining of titanium with TeflonFEP resulted in the formation of Ti-F and Ti-O bonds [11, 12]. Figure 8 illustrates the titanium side of a bulk TeflonFEP-Ti sample upon removing the polymer side. It shows that Ti-F bond was confined within the interfacial region, and the existence of TeflonFEP residue indicates the establishment of strong bond between these two materials [11]. Consequently, the joint cohesively failed in the plastic base material. However, further studies are required to establish the bond strength of different polymer to metal joints when immersed in a fluid.

Kawahito et al. [69] reported strong joint strength between glassy metal ($Zr_{55}Al_{10}Ni_5Cu_{30}$) and PET. There are essentially two features that promoted such strong joint. First, the strength can be attributed to the formation of bonds on the pre-existing zirconium oxide film,

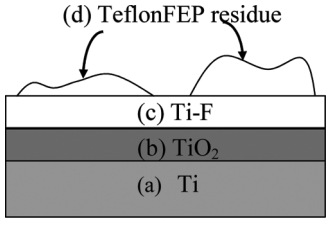

FIGURE 8.—Cross-section view of the titanium side of a bulk Ti/TeflonFEP sample after removing the polymer side [11].

TABLE 8.—Examples of combinations of metal to polymer joining.

Combination of metal and polymer	Main joint strength characteristic
Titanium and polymers [9, 15, 10, 35, 27, 11, 12, 18]	Ti-O and Ti-C chemical bonds were formed for all types of polymers, except for joining of Ti with TeflonFEP [11, 12] and KaptonFN [12], which resulted in the formation of Ti-O and Ti-F bonds.
Stainless steel (SUS304) and polymers [30, 37, 38, 48, 62]	Formation of bubbles of optimum size and quantity were responsible for strong bond in all joints. Additional bond strength is attributed to molten pool depth in [30].
Copper and polymers [30, 31]	Oxidation of copper surface increased surface roughness and heat absorptivity. This produced strong bond strength.
Al alloy and polymers [30, 32]	Anodization on the surface of Al alloy [32] and formation of molten pool with sufficient depth [30] were the sources of bond strength.
Mg alloy and polymer [28]	Formation of individual bubbles at the interfacial region produced higher bond strength than that of chains of interconnected bubbles morphology [28].

which is accompanied by growth of the oxide film [69]. Second, the X-ray diffraction (XRD) results indicate that the metal base in and near the joint was in the state of amorphousness [69]. This means that the joint retains its amorphous properties (disordered lattice structure) even after being heated. Hence, the joint cannot be easily deformed under tensile test. Some of the main characteristics of metal-polymer joint strength are summarized in Table 8.

Formation of Intermetallic Phases

Direct laser joining of metal-ceramic is often considered difficult partly due to chemical incompatibility. In brazing technique, filler materials have been adopted to bridge the mismatch in the properties of materials. However, the formation of intermetallic phases in the joint was found to be the main cause of embrittlement, as it alters the original lattice structure [78]. When subjected to mechanical deformation, two different phases within the joint region react differently thus affecting the overall joint strength. Nonetheless, numerous successful ceramic-metal joints have been reported employing brazing technique as cited by Akselsen [47] and Nascimento et al. [78].

Bauer et al. [7] studied the use of a pulsed laser to join Ti with Ytrria-stabilized TZP, using an Ag foil as a filler metal. At the interfaces of titanium/silver and silver/TZP, energy dispersive spectroscopy (EDS) analysis did not, however, reveal any formation of intermetallic phases such as TiAg phases or supersaturated β-Ti-mixed-crystals [7], which is typical of metal-ceramic brazing [78]. This could be attributed to the advantage

TABLE 9.—Examples of some successful experiments in laser lap joining of metal to ceramic.

Combination of metal and ceramic	Thickness (mm)	Optimum laser parameters	Specific processing step	Bond strength	Comment	Ref.
i) Yttria-stabilized TZP, $\alpha_{TZP} = 10.5 \times 10^{-6}/°C$ ii) Titanium, $\alpha_{Ti} = 9.18 \times 10^{-6}/°C$	i) 2.0 ii) 0.1	$\lambda = 808$ nm; $d_s = 2 \times 0.3\,mm^2$; $P = 52$ W; $p_d = 0.5$ s of 10 pulses	100 μm thick Ag as metal filler; Argon environment	–	No quantitative evaluation of bond strength. SEM image displays good interface attributed to approximately similar thermal expansion coefficients.	[7]
i) Al_2O_3-ceramic (99.4% purity) ii) Stainless-steel Kovar (54% Fe: 29% Ni: 17% Co) $\alpha_{Ko} = 5.4 \times 10^{-6}/°C$	i) 0.60 ii) 1.50	$\lambda = 1{,}064$ nm; $110 < P < 150$ W; $10 < P_d < 14\,W/cm^2$; $90 < t < 150$ s	100 μm thick Ag base filler metal (96% Ag: 4% Ti); Argon assist gas in vacuum environment	–	No quantitative evaluation of bond strength. Wetting of ceramic was increased by adding Ti in the filler metal and joining in vacuum environment. Employment of a defocused laser beam to ensure homogenous heating of the whole surface sample.	[6]
i) Pyroceram (glass-ceramic), $\alpha_{Pyro} = 0/°C$ ii) Stainless-steel Kovar (54% Fe: 29% Ni: 17% Co)	i) - ii) -	$\lambda = 10{,}640$ nm; $P_p = 315$ W; $P_R = 50$ W/min; $t = 1$ min; $3.8 < d_s < 5.1$ mm	Ag-Cu-Ti alloys as metal filler; preheated for 10 min; vacuum environment;	Passed high temperature test at 600°C and thermal shock	Nd:YAG and CO_2 lasers were used, but the latter produced the best result for Pyroceram/Kovar joint in comparison to about 30 dissimilar metal-ceramic combinations (virtually about similar thermal expansion coefficients).	[4]

of short laser processing time which limits the formation of such phases [7] and the absence of mechanical interaction which could speed up the intermixing in the molten pool. Table 9 is a list, though not exhaustive, of successful experiments in laser lap joining of metal to ceramic.

Summary and conclusion

Joining of two dissimilar materials using a laser source is still not widely employed and remains limited to certain types of material configurations that had been tested until today. The optimum experimental parameters acquired for some material configurations are not directly applicable to other joint configurations. For example, process parameters used in joining glass to ceramic cannot be employed (or precisely adapted for use) in joining glass to metal. Hence, predictability issue is one of the main concerns in this work.

To date, joint strength is mainly measured based on tensile strength. The highest tensile value would determine the optimum process parameters. However, there is lack of comprehensive relationship between joint strength and process parameters with other tests, such as fatigue, formability, static and dynamic loading, and corrosion. In addition, there is limited work that has been done to determine the optimum bond area required for successful joining experiments. This is particularly useful in manufacturing of miniature devices. Defect assessment procedures pertaining to laser lap spot joining is also needed; this is especially important in electronic and electrical components fabrication.

Application of laser lap joining of metal and ceramic in ambient conditions remains a challenge due to the demand of an inert environment posed by titanium-based filler alloys [6]. In addition, there exist inadequate literature reports on the effects of intermediate layers in laser joining of metal with glass [7, 8], which is highly required since glass is susceptible to crack as a result of thermal loading [7]. However, no work, as far as the authors are aware, has ever been reported on laser joining between ceramic and glass.

Undoubtedly, bubbles formation was found to enhance joint strength. However, a quantitative analysis of the bubble's dimension and shape for optimum joint strength remains a subject of further investigation.

Furthermore, it is noted that the achievable joint strength depends on the physical and chemical properties of the materials, laser parameters, sample preparation, and joint characteristics. This dependency can be summarized as follows:

1. Laser lap joining does not necessarily require the upper material to be transparent for the laser radiation to be effectively transmitted to the interface. When the typical lap joint configuration is reversed, the thermal conduction of an opaque material plays an important role in causing melting to occur at the interface. Sufficient clamping pressure between materials is essential to avoid ablation and non-uniform heat distribution.

2. Two materials having approximately similar thermal expansion coefficients can be easily joined. Alternatively, employment of intermediate layers was found useful to compensate for physical and chemical mismatch between dissimilar materials.
3. Sample preparation and cleaning are advantageous to positively alter the physical properties of the materials.
4. Appropriate selection of laser power/energy and scanning speed is important. For example, joining of titanium with polyimide performs better at low speed and medium power. On the contrary, strong bond of titanium and PET joint was achieved at medium speed and power. These were influenced by surface wetting of metal surface and polymer degradation.
5. Reliable bond strength is attributed to the formation of chemical bonds, optimum bubble morphology, formation of intermetallic phases, and molten pool.

Acknowledgments

The authors are grateful to the Ministry of Higher Education Malaysia for the grant (FP018-2011A) allocated to the project. The authors are thankful to Harizam Mohd Zin for his support on the project particularly during the grant application. The authors also wish to thank Khadijah Olaniyan (Loughborough University, U.K.) and Abdul Lateef Balogun (Universiti Teknologi PETRONAS, Malaysia) for helpful discussions.

References

1. Sun, Z.; Ion, J. Laser welding of dissimilar metal combinations. *Journal of Materials Science* **1995**, *30* (17), 4205–4214.
2. Katayama, S. Laser welding of aluminium alloys and dissimilar metals. *Welding International* **2004**, *18* (8), 618–625.
3. Mai, T.A.; Spowage, A.C. Characterisation of dissimilar joints in laser welding of steel-kovar, copper-steel and copper-aluminium. *Materials Science and Engineering A: Structural Materials Properties Microstructure and Processing* **2004**, *374* (1–2), 224–233.
4. Churchill, R.J.; Varshney, U.; Groger, H.P.; Glass, J.M. Laser Brazing for Ceramic-to-Metal Joining. US Patent No. 5407119A 1995.
5. Pelletier, J.M.; Robin, M. Metal-ceramic joining by laser. *Journal De Physique IV* **1993**, *3*, C7-1061-C1067-1064.
6. Haferkamp, H.; Bach, F.W.; von Alvensleben, F.; Kreutzburg, K. Laser beam active brazing of metal ceramic joints. *Proc. SPIE 2703, Lasers as Tools for Manufacturing of Durable Goods and Microelectronics*, 1996; pp. 300–309.
7. Bauer, I.; Russek, U.A.; Herfurth, H.J.; Witte, R.; Heinemann, S.; Newaz, G.; Mian, A.; Georgiev, D.; Auner, G. Laser micro-joining of dissimilar and biocompatible materials. *Proc. SPIE 5339, Photon Processing in Microelectronics and Photonics III*, July 15, 2004; pp. 454–464.
8. Ozeki, Y.; Inoue, T.; Tamaki, T.; Yamaguchi, H.; Onda, S.; Watanabe, W.; Sano, T.; Nishiuchi, S.; Hirose, A.; Itoh, K. Direct welding between copper and glass substrates with femtosecond laser pulses. *Applied Physics Express* **2008**, *1* (8).
9. Georgiev, D.G.; Baird, R.J.; Newaz, G.; Auner, G.; Witte, R.; Herfurth, H. An XPS study of laser-fabricated polyimide/titanium interfaces. *Applied Surface Science* **2004**, *236* (1–4), 71–76.
10. Georgiev, D.G.; Sultana, T.; Mian, A.; Auner, G.; Herfurth, H.; Witte, R.; Newaz, G. Laser fabrication and characterization of sub-millimeter joints between polyimide and Ti-coated borosilicate glass. *Journal of Materials Science* **2005**, *40* (21), 5641–5647.
11. Georgiev, G.L.; Baird, R.J.; McCullen, E.F.; Newaz, G.; Auner, G.; Patwa, R.; Herfurth, H. Chemical bond formation during laser bonding of Teflon (R) FEP and titanium. *Applied Surface Science* **2009**, *255* (15), 7078–7083.
12. Georgiev, G.L.; Sultana, T.; Baird, R.J.; Auner, G.; Newaz, G.; Patwa, R.; Herfurth, H. Laser bonding and characterization of Kapton FN/Ti and Teflon FEP/Ti systems. *Journal of Materials Science* **2009**, *44* (3), 882–888.
13. Georgiev, G.L.; Sultana, T.; Baird, R.J.; Auner, G.; Newaz, G.; Patwa, R.; Herfurth, H. XPS study of laser fabricated titanium/KaptonFN interfaces. *Applied Surface Science* **2008**, *254* (22), 7173–7177.
14. Mian, A.; Newaz, G.; Vendra, L.; Rahman, N.; Georgiev, D.G.; Auner, G.; Witte, R.; Herfurth, H. Laser bonded microjoints between titanium and polyimide for applications in medical implants. *Journal of Materials Science-Materials in Medicine* **2005**, *16* (3), 229–237.
15. Newaz, G.; Mian, A.; Sultana, T.; Mahmood, T.; Georgiev, D.G.; Auner, G.; Witte, R.; Herfurth, H. A comparison between glass/polyimide and titanium/polyimide microjoint performances in cerebrospinal fluid. *Journal of Biomedical Materials Research Part A* **2006**, *79A* (1), 159–165.
16. Sultana, T.; Georgiev, G.L.; Auner, G.; Newaz, G.; Herfurth, H.J.; Patwa, R. XPS analysis of laser transmission micro-joint between poly (vinylidene fluoride) and titanium. *Applied Surface Science* **2008**, *255* (5), 2569–2573.
17. Sultana, T.; Newaz, G.; Georgiev, G.L.; Baird, R.J.; Auner, G.W.; Patwa, R.; Herfurth, H.J. A study of titanium thin films in transmission laser micro-joining of titanium-coated glass to polyimide. *Thin Solid Films* **2010**, *518* (10), 2632–2636.
18. Wang, X.; Li, P.; Xu, Z.K.; Song, X.H.; Liu, H.X. Laser transmission joint between PET and titanium for biomedical application. *Journal of Materials Processing Technology* **2010**, *210* (13), 1767–1771.
19. Wild, M.J.; Gillner, A.; Poprawe, R. Locally selective bonding of silicon and glass with laser. *Sensors and Actuators A: Physical* **2001**, *93* (1), 63–69.
20. Bardin, F.; Kloss, S.; Wang, C.H.; Moore, A.J.; Jourdain, A.; De Wolf, I.; Hand, D.P. Laser bonding of glass to silicon using polymer for microsystems packaging. *Journal of Microelectromechanical Systems* **2007**, *16* (3), 571–580.
21. Shi, T.; Nie, L.; Tang, Z. Surface activated prebonding in local laser bonding of silicon and glass. *Proceedings of the 2nd IEEE International Conference on Nano/Micro Engineered and Molecular Systems*, Bangkok, Thailand, January 16–19, 2007; pp. 155–158.
22. Wu, Q.; Lorenz, N.; Hand, D.P. Localised laser joining of glass to silicon with BCB intermediate layer. *Microsystem Technologies-Micro- and Nanosystems-Information Storage and Processing Systems* **2009**, *15* (7), 1051–1057.

23. Mian, A.; Newaz, G.; Mahmood, T.; Auner, G. Mechanical characterization of glass/polyimide microjoints fabricated using cw fiber and diode lasers. *Journal of Materials Science* **2007**, *42* (19), 8150–8157.
24. Kawahito, Y.; Nishimoto, K.; Katayama, S. LAMP joining between ceramic and plastic. *Physics Procedia* **2011**, *12*, 174–178.
25. Najafi, K. Packaging of implantable microsystems. *IEEE Sensors* **2007**, *1–3*, 58–63.
26. Mian, A.; Sultana, T.; Georgiev, D.; Witte, R.; Herfurth, H.; Auner, G.; Newaz, G. Postimplantation pressure testing and characterization of laser bonded glass/polyimide microjoints. *Journal of Biomedical Materials Research Part B: Applied Biomaterials* **2009**, *90B* (2), 614–620.
27. Patwa, R.; Herfurth, H.; Heinemann, S.; Ehrenmann, S.; Newaz, G.; Baird, R.J. Fiber laser microjoining for novel dissimilar material combinations. *Proc. SPIE 7202, Laser-Based Micro- and Nanopackaging and Assembly III*, March 12, 2009.
28. Wahba, M.; Kawahito, Y.; Katayama, S. Laser direct joining of AZ91D thixomolded Mg alloy and amorphous polyethylene terephthalate. *Journal of Materials Processing Technology* **2011**, *211* (6), 1166–1174.
29. Wang, X.; Song, X.H.; Jiang, M.F.; Li, P.; Hu, Y.; Wang, K.; Liu, H.X. Modeling and optimization of laser transmission joining process between PET and 316 L stainless steel using response surface methodology. *Optics and Laser Technology* **2012**, *44* (3), 656–663.
30. Yusof, F.; Miyashita, Y.; Hua, W.; Mutoh, Y.; Otsuka, Y. YAG laser spot welding of PET and metallic materials. *Journal of Laser Micro Nanoengineering* **2011**, *6* (1), 69–74.
31. Yusof, F.; Mutoh, Y.; Miyashita, Y. Effect of pre-oxidized CuO layer in joining between polyethylene terephalate (PET) and copper (Cu) by using pulsed Nd:YAG laser. *Advanced Materials Research* **2010**, *129–131*, 714–718.
32. Yusof, F.; Yukio, M.; Yoshiharu, M.; Shukor, M.H.A. Effect of anodizing on pulsed Nd:YAG laser joining of polyethylene terephthalate (PET) and aluminium alloy (A5052). *Materials and Design* **2012**, *37*, 410–415.
33. Grewell, D.; Benatar, A. Welding of plastics: Fundamentals and new developments. *International Polymer Processing* **2007**, *22* (1), 43–60.
34. Amanat, N.; James, N.L.; McKenzie, D.R. Welding methods for joining thermoplastic polymers for the hermetic enclosure of medical devices. *Medical Engineering and Physics* **2010**, *32* (7), 690–699.
35. Mian, A.; Sultana, T.; Auner, G.; Newaz, G. Bonding mechanisms of laser-fabricated titanium/polyimide and titanium coated glass/polyimide microjoints. *Surface and Interface Analysis* **2007**, *39* (6), 506–511.
36. Wu, Q.; Lorenz, N.; Cannon, K.M.; Hand, D.P. Glass frit as a hermetic joining layer in laser based joining of miniature devices. *IEEE Transactions on Components and Packaging Technologies* **2010**, *33* (2), 470–477.
37. Fortunato, A.; Cuccolini, G.; Ascari, A.; Orazi, L.; Campana, G.; Tani, G. Hybrid metal-plastic joining by means of laser. *International Journal of Material Forming* **2010**, *3*, 1131–1134.
38. Tillmann, W.; Elrefaey, A.; Wojarski, L. Toward process optimization in laser welding of metal to polymer. *Materialwissenschaft Und Werkstofftechnik* **2010**, *41* (10), 879–883.
39. Gower, H.L.; Pieters, R.R.G.M.; Richardson, I.M. Pulsed laser welding of metal-polymer sandwich materials using pulse shaping. *Journal of Laser Applications* **2006**, *18* (1), 35–41.
40. Holtkamp, J.; Roesner, A.; Gillner, A. Advances in hybrid laser joining. *International Journal of Advanced Manufacturing Technology* **2010**, *47* (9–12), 923–930.
41. Bassani, P.; Capello, E.; Colombo, D.; Previtali, B.; Vedani, M. Effect of process parameters on bead properties of A359/SiC MMCs welded by laser. *Composites Part A: Applied Science and Manufacturing* **2007**, *38* (4), 1089–1098.
42. Watanabe, W.; Onda, S.; Tamaki, T.; Itoh, K.; Nishii, J. Space-selective laser joining of dissimilar transparent materials using femtosecond laser pulses. *Applied Physics Letters* **2006**, *89* (2), 021106.
43. Luo, C.; Lin, L.W. The application of nanosecond-pulsed laser welding technology in MEMS packaging with a shadow mask. *Sensors and Actuators A: Physical* **2002**, *97–98*, 398–404.
44. Mescheder, U.M.; Alavi, M.; Hiltmann, K.; Lietzau, C.; Nachtigall, C.; Sandmaier, H. Local laser bonding for low temperature budget. *Sensors and Actuators A: Physical* **2002**, *97–98*, 422–427.
45. Watanabe, W.; Tamaki, T.; Itoh, K. Ultrashort laser welding and joining. In *Femtosecond Laser Micromachining*; Osellame, R.; Cerullo, G.; Ramponi, R., Eds.; Springer: Berlin, Heidelberg, **2012**; 467–477.
46. Watanabe, W.; Onda, S.; Tamaki, T.; Itoh, K. Direct joining of glass substrates by 1 kHz femtosecond laser pulses. *Applied Physics B: Lasers and Optics* **2007**, *87* (1), 85–89.
47. Akselsen, O.M. Advances in Brazing of Ceramics. *Journal of Materials Science* **1992**, *27* (8), 1989–2000.
48. Katayama, S.; Kawahito, Y. Laser direct joining of metal and plastic. *Scripta Materialia* **2008**, *59* (12), 1247–1250.
49. Tan, A.W.Y.; Tay, F.E.H. Localized laser assisted eutectic bonding of quartz and silicon by Nd:YAG pulsed-laser. *Sensors and Actuators A: Physical* **2005**, *120* (2), 550–561.
50. Miyashita, Y.; Takahashi, M.; Takemi, M.; Oyama, K.; Mutoh, Y.; Tanaka, H. Dissimilar materials micro welding between stainless steel and plastics by using pulsed YAG laser. *Journal of Solid Mechanics and Materials Engineering* **2009**, *3* (2), 409–415.
51. Zakariyah, S.S.; Conway, P.P.; Hutt, D.A.; Selviah, D.R.; Wang, K.; Rygate, J.; Calver, J.; Kandulski, W. Fabrication of polymer waveguides by laser ablation using a 355 nm wavelength Nd: YAG laser. *Journal of Lightwave Technology* **2011**, *29* (23), 3566–3576.
52. Meijer, J. Laser beam machining (LBM), state of the art and new opportunities. *Journal of Materials Processing Technology* **2004**, *149* (1), 2–17.
53. Dubey, A.K.; Yadava, V. Laser beam machining: A review. *International Journal of Machine Tools and Manufacture* **2008**, *48* (6), 609–628.
54. Gillner, A.; Holtkamp, J.; Hartmann, C.; Olowinsky, A.; Gedicke, J.; Klages, K.; Bosse, L.; Bayer, A. Laser applications in microtechnology. *Journal of Materials Processing Technology* **2005**, *167* (2), 494–498.
55. Qi, H.; Chen, T.; Yao, L.; Zuo, T. Micromachining of microchannel on the polycarbonate substrate with CO_2 laser direct-writing ablation. *Optics and Lasers in Engineering* **2009**, *47* (5), 594–598.

56. Zakariyah, S.S.; Conway, P.P.; Hutt, D.A.; Wang, K.; Selviah, D.R. CO_2 laser micromachining of optical waveguides for interconnection on circuit boards. *Optics and Lasers in Engineering* **2012**, *50* (12), 1752–1756.
57. Witte, R.; Herfurth, H.; Bauer, I. Microjoining of dissimilar materials for optoelectronic and biomedical applications *Proc. SPIE 4979, Micromachining and Microfabrication Process Technology VIII*, January 15, 2003, 226–233.
58. Theppakuttai, S.; Shao, D.; Chen, S. Localized laser transmission bonding for microsystem fabrication and packaging. *Journal of Manufacturing Processes* **2004**, *6* (1), 24–31.
59. Tamaki, T.; Watanabe, W.; Nishii, J.; Itoh, K. Welding of transparent materials using femtosecond laser pulses. *Japanese Journal of Applied Physics* **2005**, *44* (20–23), L687–L689.
60. Chan, J.W.; Huser, T.; Risbud, S.; Krol, D.M. Structural changes in fused silica after exposure to focused femtosecond laser pulses. *Opt. Lett.* **2001**, *26* (21), 1726–1728.
61. Watanabe, W.; Tamaki, T.; Ozeki, Y.; Itoh, K. Filamentation in ultrafast laser material processing. In *Progress in Ultrafast Intense Laser Science VI*; Yamanouchi, K.; Gerber, G.; Bandrauk, A.D., Eds.; Springer: Berlin Heidelberg, 2010; 161–181.
62. Roesner, A.; Scheik, S.; Olowinsky, A.; Gillner, A.; Reisgen, U.; Schleser, M. Laser assisted joining of plastic metal hybrids. *Physics Procedia* **2011**, *12*, 370–377.
63. Amancio, S.T.; dos Santos, J.F. Joining of polymers and polymer-metal hybrid structures: Recent developments and trends. *Polymer Engineering and Science* **2009**, *49* (8), 1461–1476.
64. Albaugh, K.B. Electrode phenomena during anodic bonding of silicon to sodium borosilicate glass. *Journal of the Electrochemical Society* **1991**, *138* (10), 3089–3094.
65. Cao, X.; Jahazi, M.; Immarigeon, J.P.; Wallace, W. A review of laser welding techniques for magnesium alloys. *Journal of Materials Processing Technology* **2006**, *171* (2), 188–204.
66. Zakariyah, S.S.; Conway, P.P.; Hutt, D.A.; Selviah, D.R.; Wang, K.; Baghsiahi, H.; Rygate, J.; Calver, J.; Kandulski, W. Polymer optical waveguide fabrication using laser ablation. 11th Electronics Packaging Technology Conference, 2009, 936–941.
67. Lubna, N.; Auner, G.; Patwa, R.; Herfurth, H.; Newaz, G. Role of cleaning methods on bond quality of Ti coated glass/imidex system. *Applied Surface Science* **2011**, *257* (10), 4749–4753.
68. You, B.; Park, W.; Chung, I. The effect of calcium additions on the oxidation behavior in magnesium alloys. *Scripta Materialia* **2000**, *42* (11), 1089–1094.
69. Kawahito, Y.; Niwa, Y.; Terajima, T.; Katayama, S. Laser direct joining of glassy metal $Zr_{55}Al_{10}Ni_5Cu_{30}$ to engineering plastic polyethylene terephthalate. *Materials Transactions* **2010**, *51* (8), 1433–1436.
70. Xiao, Z.X.; Wu, G.Y.; Li, Z.H.; Zhang, C.B.; Hao, Y.L.; Wang, Y.Y. Silicon-glass wafer bonding with silicon hydrophilic fusion bonding technology. *Sensors and Actuators A: Physical* **1999**, *72* (1), 46–48.
71. Tseng, A.A.; Park, J.S. Mechanical strength and interface characteristics of transmission laser bonding. *IEEE Transactions on Electronics Packaging Manufacturing* **2006**, *29* (3), 191–201.
72. Haberstroh, E.; Hoffmann, W.-M.; Poprawe, R.; Sari, F. 3 Laser transmission joining in microtechnology. *Microsystem Technologies* **2006**, *12* (7), 632–639.
73. Gillner, A.; Wild, M.; Poprawe, R. Laser bonding of micro-optical components. *Proc. SPIE 4941, Laser Micromachining for Optoelectronic Device Fabrication*, April 18, 2003; pp. 112–120.
74. Lubna, N.; Newaz, G. Analysis of titanium-coated glass and Imidex (PI) laser bonded samples. *Journal of Materials Engineering and Performance* **2012**, *21* (2), 266–270.
75. Lubna, N. Laser bonding characteristics of sputtered titanium on glass with polymeric films. Ph.D. dissertation, Wayne State University, 2009.
76. Knechtel, R. Glass frit bonding: An universal technology for wafer level encapsulation and packaging. *Microsystem Technologies-Micro- and Nanosystems-Information Storage and Processing Systems* **2005**, *12* (1–2), 63–68.
77. Massey, L.K. *Permeability Properties of Plastics and Elastomers: A Guide to Packaging and Barrier Materials*; William Andrew Publishing: New York, 2002; 205.
78. Nascimento, R.M.D.; Martinelli, A.E.; Buschinelli, A.J.A. Review article: Recent advances in metal-ceramic brazing. *Cerâmica* **2003**, *49*, 178–198.
79. Ready, J.F.; Farson, D.F. *LIA Handbook of Laser Materials Processing*; Laser Institute of America: Orlando, USA, 2001; 182.